

# MOLECULAR STRUCTURE ANALYSIS AND SPECTROSCOPIC CHARACTERIZATION OF 1,5-DINITRONAPHTHALENE WITH EXPERIMENTAL (FT-IR AND FT-RAMAN) TECHNIQUES AND QUANTUM CHEMICAL CALCULATIONS

J.Amirtha selva mary<sup>1</sup>, D.Mohan radheep<sup>1</sup> and K.Sambathkumar<sup>2</sup>

<sup>1</sup> R& D centre, Ponnaiyah Ramajayam Institute of science and Technology, Puducherry campus, Puducherry, India.

<sup>2</sup> P.G.& Research Department of Physics, (Computational and Theoretical Divisions), A.A.Govt.Arts College, Villupuram, India.

**Abstract**— The FT-IR and FT-Raman spectra of DNN were recorded in the solid phase. The molecular geometry and vibrational frequencies of 1,5-dinitronaphthalene (DNN) in the ground state have been calculated by using the density functional methods (B3LYP) invoking 6-311+G(d,p) and 6-311++G(d,p) basis set. The optimized geometric bond lengths and bond angles obtained by DFT method show best agreement with the experimental values. NBOs are localized electron pair orbitals for bonding pairs and lone pairs. HOMO and LUMO energies were performed by time dependent density functional theory (TD-DFT) approach. Finally the calculations results were applied to simulated infrared and Raman spectra of the title compound which show good agreement with observed spectra. And the temperature dependence of the thermodynamic properties of constant pressure ( $C_p$ ), entropy ( $S$ ) and enthalpy change ( $\Delta H_0$ ) for DNN were also determined.

**Keywords:** DNN, HOMO- LUMO, NBO, MEP.

## I. INTRODUCTION

Naphthalene and its derivatives are biologically, pharmaceutically and industrially useful compounds. The structure of naphthalene is benzene-like, having two-six membered rings fused together. Particularly, naphthalene was studied because, of its technological applications in a vast amount of industrial process. In fact, it was used as a precursor for the synthesis of plastics and dyes, gamma-ray detector in photomultiplier tubes and also used in dye stuffs, synthetic resins, coatings, tanning agent and celluloid. The vibrational analysis of the 1,5-dinitronaphthalene (DNN) of normal coordinate analysis based on semi-empirical methods. Modern vibrational spectrometry has proven to be an exceptionally powerful technique for solving many chemical problems. It has been extensively employed both in the study of chemical kinetics and chemical analysis. The problem of signal assignment however, as well as understanding the relationship between the observed spectral features and molecular structure, and reactivity can be difficult. Even identification of fundamental vibrational frequencies often generates controversy. However, for a proper understanding of IR and Raman, a reliable assignment of all vibrational band is essential. Recently, computational methods based on density functional theory (DFT) are becoming widely used. These methods predict relatively accurate molecular structure and vibrational spectra with moderate computational effort. In particular, for polyatomic molecules (typically normal modes exceeding 50) the DFT methods lead to the prediction of more accurate molecular structure and vibrational frequencies

than the conventional ab initio and restricted Hartree-Fock (RHF) calculations. Among the DFT calculation, Becke's three parameter hybrid functional combined with the Lee-Yang-Parr correlation functional (B3LYP) is the best in predicting results for molecular geometry and vibrational wave numbers for moderately larger molecules [1-6]. To gain a better understanding of the performance and limits of DFT methods as a general approach to the vibrational problems of organic molecules, the calculated harmonic frequencies of 1,5-dinitronaphthalene (DNN) by DFT method, and compared these results with observed fundamental vibrational frequencies. The aim of this work is to check the performance of B3LYP density functional force field for simulation of IR and Raman spectra of the title compounds with the use of standard 6-311+G(d,p) and 6-311++G(d,p) basis sets (referred to as small and large basis set, respectively). The simulated and observed spectra were analysed in detail. In addition HOMO, LUMO analysis has been used to elucidate the information regarding charge transfer within the molecule.

## II EXPERIMENTAL

The fine polycrystalline samples of DNN were obtained from the Lancaster Chemical Company, UK and used as such for the spectral measurements. The room temperature Fourier transform infrared spectra of the title compounds were measured in the 4000-50  $\text{cm}^{-1}$  region at a resolution of  $\pm 1 \text{ cm}^{-1}$  using a BRUKER IFS-66V FTIR spectrometer equipped with dual detection : a cooled MCT detector for the mid-IR and a room temperature pyroelectric detector for the far-IR range. KBr and

polyethylene pellets were used in the spectral measurements. Boxcar apodization was used for the 250 averaged interferograms collected for both the sample and background. The FT-Raman spectra of DNN were recorded on a BRUKER IFS-66V model interferometer equipped with an FRA-106 FT-Raman accessory in the 3500-100  $\text{cm}^{-1}$  Stokes region using the 1064 nm line of a Nd:YAG laser for excitation operating at 200 mW power. The reported wave numbers are believed to be accurate within  $\pm 1 \text{ cm}^{-1}$ .

### III COMPUTATIONAL DETAILS

The molecular geometry optimizations, energy and vibrational frequency calculations were carried out for DNN with the GAUSSIAN-09 software package [7] using the B3LYP functionals [8,9] combined with the standard 6-311+G(d,p) and 6-311++G(d,p) basis sets. The theoretical force constants have been computed at optimized geometry by assuming  $C_s$  point group symmetry. Scaling of the force field was performed according to the SQM procedure [10] using selective scaling in the natural internal coordinate representation. Transformations of the force field and the subsequent normal coordinate analysis including the least square refinement of the scaling factors, calculation of the total energy distribution (TED), and the prediction of IR and Raman intensities were done on a PC with the MOLVIB program (Version V 7.0 - G77) written by Sundius [11]. The symmetry of the molecule was also helpful in making vibrational assignments. The symmetries of the vibrational modes were determined by using the standard procedure of decomposing the traces of the symmetry operation into the irreducible representations. The symmetry analysis for the vibrational modes of DNN are presented in some details in order to describe the basis for the assignments. By combining the results of the GAUSSVIEW program [12] with symmetry considerations, vibrational frequency assignments were made with a high degree of confidence. There is always some ambiguity in defining internal coordination. However, the defined coordinate form complete set and matches quite well with motions observed using the GAUSSVIEW program.

#### III.I Prediction of Raman intensities

The Raman activities ( $S_i$ ) calculated with the GAUSSIAN-09 program and adjusted during the scaling procedure with MOLVIB were subsequently converted to relative Raman intensities ( $I_i$ ) using the following relationship derived from the basic theory of Raman scattering [13].

$$I_i = \frac{f(v_0 - v_i)^4 S_i}{v_i \left[ 1 - \exp\left(\frac{hc v_i}{kT}\right) \right]}$$

where  $v_0$  is the exciting frequency (in  $\text{cm}^{-1}$  units),  $v_i$  is the vibrational wave number of the  $i^{\text{th}}$  normal mode,  $h$ ,  $c$  and  $k$  are fundamental constants and  $f$  is a suitably chosen common normalization factor for all peak intensities.

### IV RESULTS AND DISCUSSION

#### IV.1 Molecular geometry

The optimized molecular structures of DNN obtained from GAUSSIAN 09 and GAUSSVIEW programs are shown in Fig.1, respectively. The detailed description of vibrational modes can be given by means of

normal coordinate analysis (NCA). For this purpose the full set of 81 standard internal coordinates (containing 21 redundancies) for DNN, respectively, were defined as given in Table 1, that are bond length, bond angle respectively. From these, a non-redundant set of local symmetry coordinates were constructed by suitable linear combinations of internal coordinates following the recommendations of Fogarasi and Pulay [14] are summarised in Tables 2 and 3. The theoretically calculated DFT force fields were transformed to this latter set of vibrational coordinates and used in all subsequent calculations.

#### V VIBRATIONAL SPECTRA

The 60 normal modes of DNN are distributed amongst the symmetry species as

$$\Gamma_{3N-6} = 41A'(\text{in-plane}) + 19A''(\text{out-of-plane})$$

in agreement with  $C_s$  symmetry. All the vibrations are active both in the Raman scattering and infrared absorption. The detailed vibrational assignment of fundamental modes of DNN along with the calculated IR and Raman intensities and normal mode descriptions (characterized by TED) and reported in Table 4. For visual comparison, the observed and simulated FTIR and FT-Raman spectra of DNN are presented in Figs. 2 and 3, respectively, which helps to understand the observed spectral features.

#### VI Effect of scaling on frequency fit and assignment

The vibrational frequencies obtained by DFT calculations are known for over estimation from the experimental values by 2-7% on average. This is so in case of both DNN as well as reflected in Tables 8 with the RMS frequency error being 69.71 and 83.93  $\text{cm}^{-1}$ , respectively. A tentative assignment is often made on the basis of unscaled frequencies by assuming the observed frequencies so that they are in the same order as the calculated ones. Then, for an easier comparison to the observed values, the calculated frequencies are scaled by the scale to less than 1, to minimize the overall deviation. An attempt was made to refine the scale factors, using the set of transferable scale factors (for actual values see Table 3). In order to reproduce the observed frequencies, the refinement of scaling factors were applied and optimized via least square refinement algorithm, which resulted a weighted RMS deviation of 7.20 and 3.16  $\text{cm}^{-1}$  for DNN, respectively, for the B3LYP/6-311+G(d,p)(small) and 6-311++G(d,p) (large) basis sets between experimental and SQM frequencies.

#### Nitro groups vibrations

The characteristics group frequencies of the nitro group are relatively independent of the rest of the molecule which makes this group convenient to identify. For the assignments of  $\text{NO}_2$  group frequencies basically six fundamentals can be associated to each  $\text{NO}_2$  group namely,  $\text{NO}_2$  ss - symmetric stretch;  $\text{NO}_2$  ass - antisymmetric stretch;  $\text{NO}_2$  sciss - scissoring; and  $\text{NO}_2$  rock - rocking which are belongs to in-plane ( $A'$ ) vibrations. In addition to that  $\text{NO}_2$  wag - wagging and  $\text{NO}_2$  twist - twisting modes of  $\text{NO}_2$  group would be expected to be depolarised for out-of-plane ( $A''$ ) symmetry species. The antisymmetric  $\text{NO}_2$  stretching vibrations are generally observed in the region 1570-1485

$\text{cm}^{-1}$ , while the symmetric stretch will appear between  $1370 - 1320 \text{ cm}^{-1}$  [15]. The  $\text{NO}_2$  antisymmetric vibrations were observed in IR and Raman spectra at  $1605$  and  $1567 \text{ cm}^{-1}$ , respectively for DNN. The symmetric stretching were also identified in Raman and IR spectra at  $1352$  and  $1347 \text{ cm}^{-1}$  for DNN. The bands corresponding to scissoring, rocking, wagging and twisting vibrations of  $\text{NO}_2$  group were also found well within the characteristic region and are summarised in Table 4. These assignments are also supported by TED.

#### Carbon-Nitrogen vibrations

The IR and Raman bands appeared at  $1475$  and  $1459 \text{ cm}^{-1}$  in DNN have been designated to C-N stretching vibrations. The in-plane and out-of-plane bending vibrations assigned in this study are also supported by the literature [16]. The identification of C-N vibration is a difficult task since, it falls in a complicated region of the vibrational spectrum. However, with the help of force field calculations, the C-N vibrations were identified and assigned in this study.

#### Carbon-Nitrogen vibrations

The IR and Raman bands appeared at  $1475$  and  $1459 \text{ cm}^{-1}$  in DNN have been designated to C-N stretching vibrations. The in-plane and out-of-plane bending vibrations assigned in this study are also supported by the literature [16]. The identification of C-N vibration is a difficult task since, it falls in a complicated region of the vibrational spectrum. However, with the help of force field calculations, the C-N vibrations were identified and assigned in this study.

#### Carbon – Hydrogen vibrations

THE HETEROATOMIC STRUCTURE SHOWS THE PRESENCE OF C–H STRETCHING VIBRATIONS IN THE REGION  $3000-3100 \text{ CM}^{-1}$  WHICH IS THE CHARACTERISTIC REGION FOR THE READY IDENTIFICATION OF SUCH C–H STRETCHING VIBRATIONS [17]. ACCORDINGLY, IN THE PRESENT STUDY, THE C-H VIBRATIONS OF THE TITLE COMPOUND ARE OBSERVED AT  $3100, 3050, 2992$  AND  $2988 \text{ CM}^{-1}$  IN THE FT-IR SPECTRUM AND AT  $3084$  AND  $3064 \text{ CM}^{-1}$  IN THE RAMAN FOR DNN.

#### VII HOMO-LUMO energy gap

The energy levels of the frontier orbital of the compound are listed in Table 5. The 3D plots of the HOMOs and LUMOs of the compound are shown in Fig.4. The positive phase is red and the negative one is green. It is clear from the Fig. 4 that, while the HOMO localizes on the three bond regions (C1–N11, C5–N17), a highly delocalized HOMO and LUMO indicates that the electrons can more readily move around the molecule and hence an improved ICT. On the other hand, the LUMO strongly localizes on the five different bond regions indicating the presence of favorable atomic centers within DNN for possible electrophilic attacks and its bioactivity. The HOMO-LUMO energies and other related properties of energy gap, ionization potential (I), the electron affinity (A), the absolute electronegativity ( $\chi$ ), the absolute hardness ( $\eta$ ) and softness (S) for the DNN molecule have been calculated and values are given in table 5. The molecular energy transfer of DNN compound is shown in Fig 4. HOMO and LUMO energy values for a molecule,

electronegativity and chemical hardness can be calculated

as follow:  $\chi = \frac{I+A}{2}$  (Electronegativity)

$$\mu = -\frac{(I+A)}{2} \text{ (Chemical potential)}$$

$$\eta = \frac{I-A}{2} \text{ (Chemical hardness)}$$

$$s=1/2\eta \text{ (chemical softness), } \omega=\mu^2/2\eta \text{ (Electrophilicity index)}$$

Where I and A are ionization potential and electron affinity;  $I = -E_{\text{HOMO}}$  and  $A = -E_{\text{LUMO}}$  respectively. The ground state (HOMO) energy is  $-6.9795 \text{ eV}$  and the first excited state (LUMO) energy is  $-2.8564 \text{ eV}$ . The ground state and first excited state energy gap of DNN is found to be  $4.1231 \text{ eV}$ . Hence, the energy gap of title compound DNN is low. This energy gap is elucidate the eventual charge transfer occur within the molecule.

#### VIII Non-linear optical analysis

In discussing nonlinear optical properties, the polarization of the molecule by an external radiation field is often approximated as the creation of an induced dipole moment by an external electric field. Under the weak polarization condition, we can use a Taylor series expansion in the electric field components to demonstrate the dipolar interaction with the external radiation electric field. The first order hyperpolarizability ( $\beta_{\text{total}}$ ) of this novel molecular system the related properties ( $\mu$ ,  $\alpha$  and  $\Delta\alpha$ ) of DNN were investigated by DFT/ Becke-3-Lee-Yang-Parr method with 6-311++G(d,p) basis set, is based on the finite-field approach. In the presence of an applied electric field, the energy to a system is a function of the electric field. Nonlinear optical effects (NLO) is at the forefront of the recent investigation because of its significance in bestowing the key functions of optical modulation, optical logic, optical memory, optical switching and frequency shifting for the presently growing technologies in areas such as telecommunications, signal processing, and optical interconnections. The non-linear optical response of an isolated molecule in an electric field  $E_i(\omega)$  can be represented as a Taylor series enlargement of the total dipole moment,  $\mu_{\text{tot}}$ , induced by the field:

$$\mu_{\text{tot}} = \mu_0 + \alpha_{ij} E_j + \beta_{ijk} E_j E_k + \dots$$

Where  $\alpha$  is the linear polarizability,  $\mu_0$  is the permanent dipole moment and  $\beta_{ijk}$  are the first hyperpolarizability tensor components. The isotropic (or average) linear polarizability is defined as:

$$\alpha = \frac{\alpha_{xx} + \alpha_{yy} + \alpha_{zz}}{3}$$

The first order hyperpolarizability is a third rank tensor that can be described by  $3 \times 3 \times 3$  matrix. The 27 components of 3D matrix can be abridged to 10 components owing to the Kleinman symmetry [20]

.Components of the first hyperpolarizability can be reckoned using the following equation. Using the x, y and z components of  $\beta$ , the magnitude of the first hyperpolarizability tensor can be calculated by:

$$\beta_{\text{tot}} = \sqrt{(\beta_x^2 + \beta_y^2 + \beta_z^2)}$$

The entire equation for reckoning the magnitude of  $\beta$  from Gaussian 09W program output is given a follows:

$$\beta_{tot} = \sqrt{(\beta_{xxx} + \beta_{yyy} + \beta_{zzz})^2 + (\beta_{yyy} + \beta_{zzz} + \beta_{xxy})^2 + (\beta_{zzz} + \beta_{xzx} + \beta_{yyz})^2}$$

The calculations of the total molecular dipole moment ( $\mu$ ), linear polarizability ( $\alpha$ ) and first-order hyperpolarizability ( $\beta$ ) from the Gaussian output have been explained in detail previously, and DFT has been widely used as an efficient method to investigate the organic NLO materials. In addition, the polar properties of the DNN were computed at the DFT (B3LYP)/6-311++G(d,p) level using Gaussian 09W program package. Urea is the prototypical molecule utilized in investigating of the NLO properties of the compound. For this reason, urea was used often as a threshold value for comparative purpose. The calculated dipole moment and hyperpolarizability values obtained from B3LYP/6-311++G(d,p) methods are collected in Table 7. The first order hyperpolarizability of DNN with B3LYP/6-311++G(d,p) basis set is  $15.7740 \times 10^{-30}$  twenty five times greater than the value of urea ( $\beta_o = 0.6230 \times 10^{-30}$  esu). This is evidence for the good nonlinear optical (NLO) property of the molecule.

#### 1X Molecular electrostatic potential (MEP)

The molecular electrostatic potential is related to the electronic density and is a very useful descriptor for determining the sites for electrophilic and nucleophilic reactions as well as hydrogen bonding interactions [21]. To predict reactive sites of electrophilic or nucleophilic attack for the investigated molecule, the MEP at the B3LYP/6-311++G(d,p) optimized geometry was calculated. The various values of the electrostatic potential at the surface are represented by various colors. The color scheme for the MEP surface is red-electron rich, partially negative charge (electrophilic reactive center); blue-electron deficient, partially positive charge; light blue-slightly electron deficient region (nucleophilic reactive center); yellow-slightly electron rich region; green-neutral, respectively. The potential increases in the order red < orange < yellow < green < cyan < blue. It can be seen that the negative regions are mainly over the N atoms. The negative (red and yellow) regions of the MEP are related to electrophilic reactivity and the positive (blue) regions to nucleophilic reactivity, as shown in Fig.5-7. As can be seen from the figure, this molecule has several possible sites, C and N atoms for electrophilic attack.

#### X THERMODYNAMIC PROPERTIES

Standard statistical thermodynamics function, heat capacity, entropy and enthalpy changes were computed at B3LYP/6-311++G(d,p) basis set by using perl script THERMO.PL [22] and are listed in Table 8. Thermodynamic functions are all values increasing with temperature ranging from 100 to 1000K due to the fact that the molecular vibrations intensities increase with temperature. The correlation equation among heat capacities, entropies, enthalpy changes with temperatures were fitted by quadratic formulas and the corresponding fitting factors ( $R^2$ ) these thermodynamic properties are 0.9993, 0.9999 and 0.9992 respectively. The correlations plot of those shown in Fig 8. The thermodynamic correlation fitting equation is follows:

$$\left( C_{p,m}^o \right) = 25.1184 + 0.8517T - 3.8880 \times 10^{-4}T^2$$

$$\left( S_m^o \right) = 265.1208 + 0.9822T - 2.6108 \times 10^{-4}T^2$$

$$\left( H_m^o \right) = -11. + 2.1171 \times 10^{-4}T^2$$

All thermodynamic data provide useful information for further studies. to compute other thermodynamic energies according to relationships of thermodynamic functions and estimate directions of chemical reactions according to the second law of thermodynamics in thermo chemical field. Notice: all thermodynamic calculations were done in gas phase and they are not valid in solution.

#### 6. CONCLUSION

Based on the SQM force field obtained by DFT calculations at B3LYP/6-311+G(d,p) and B3LYP/6-311+G(d,p) levels, the complete vibrational properties of DNN have been investigated. The role of nitro and other groups in the vibrational frequencies of the title compounds has been discussed. The various modes of vibrations have unambiguously been assigned based on the results of the TED output obtained from normal coordinate analysis. The molecular structure, vibrational frequencies and HOMO, LUMO, DNN have been studied using DFT calculation. NBO analysis has been performed on DNN molecule in order to elucidate intermolecular hydrogen bonding, intermolecular charge transfer (ICT), rehybridization, delocalization of electron density and cooperative effect due to  $L(N) \rightarrow \pi^*(C-C)$ . Temperature dependence of the thermodynamic properties heat capacity at constant pressure ( $C_p$ ), entropy (S) and enthalpy change ( $\Delta H_0$ ) for DNN were also determined. The theoretically constructed FT-IR and FT-Raman spectrum shows good correlation with experimentally observed FT-IR and FT-Raman spectrum.

#### REFERENCE

- [1] P.Pulay, G.Fogarasi, X.Zhou, P.W. Taylor, Vib. Spectrosc. **1** (1990) 159.
- [2] H.A. Kramers, W.Heisenberg, Z.Phys. **31** (1925) 681
- [3] J.M.L. Martin, C.V. Alsenoy, J.Phys. Chem. **100** (1996) 6973
- [4] J.M.L. Martin, J.El. Yazal, J.P. Francis, J.Phys. Chem **100** (1996) 15358.
- [5] Zhou Zhengyu. Du. Dongmet. J.Mol. struct (Theochem.) **505** (2000) 247.
- [6] Zhou Zhengyu. Fu Aiping. Du. Nongmei Int.J. Quant. Chem.. **78** (2000) 186.
- [7] M. J. Frisch, G. W. Trucks, H. B. Schlegel, G. E. Scuseria, M. A. Robb, Gaussian 09, Revision E.01, Gaussian, Inc., Wallingford CT, 2009.
- [8] A.D. Becke, J. Chem. Phys., **98** (1993) 5648.
- [9] C. Lee, W. Yang, R.G. Parr, Phys. Rev., **B37** (1988) 785.
- [10] P. Pulay, G. Fogarasi, G. Pongor, J.E. Boggs, A. Vargha, J. Am. Chem. Soc. **105** (1983) 7037.
- [11] T. Sundius, J. Mol. Spectrosc. **82** (1980) 138.
- [12] GaussView, Version 5, Roy Dennington, Todd Keith, and John Millam, *Semichem Inc.*, Shawnee Mission, KS, 2009.
- [13] D.Cecily Mary Glory, R.Madivanane, K.Sambathkumar, A.Claude and K.Settu Elixir Vib. Spec. **90** (2016) 37416-37430 37416.
- [14] T.Sundius, J.Mol. Struct, **218** (1990) 321 (MOLVIB (V.7.0) : Calculation of Harmonic Force Fields and Vibrational Modes of Molecules, QCPE program No.807 (2002).
- [15] K.Parivathini, S.Manimaran and K.Sambathkumar, K.Settu and A. Claude Elixir Computational Physics **102** (2017) 44325-44336.
- [16] K.C. Medhi, R.Barman, M.K. Sharma, Indian J.Phys. **68** (1994) 189.

[17] D.Cecily Mary Glory, R.Madivanane & K.Sambathkumar Indian journal of pure and Applied Physics. Vol 55 2017( 638-648).

[18] E.D. Glendening, A.E. Reed, J.E. Carpenter, F. Weinhold, NBO Version 3.1, TCI, University of Wisconsin, Madison, 1998.

[19] A.E. Reed, L.A. Curtis, F. Weinhold, Chem. Rev. 88 (1988) 899–926.

[20] S.Manimarana, S.Jeyavijayan and K.Sambathkumar IJARMPS Vol.2,(2017) 2455-6998.

**Table 1**  
**Optimized geometrical parameters of 1,5-dinitronaphthalene obtained by B3LYP/6-311+G\*\* density functional calculations**

Bond length	Value (Å)
C1-C2	1.40
C2-C3	1.40
C3-C4	1.40
C4-C10	1.40
C10-C9	1.40
C9-C1	1.40
C10-C5	1.40
C5-C6	1.40
C6-C7	1.40
C7-C8	1.40
C8-C9	1.40
C1-N11	1.47
N11-O12	1.36
N11-O13	1.36
C2-H14	1.07
C3-H15	1.07
C4-H16	1.07
C5-H17	1.47
N17-O18	1.36
N17-O19	1.36
C6-H20	1.07
C7-H21	1.07
C8-H22	1.07
Bond angle	Value (°)
C1-C2-C3	120.00
C2-C3-C4	120.00
C3-C4-C10	120.30
C4-C10-C9	120.00
C10-C9-C1	119.40
C9-C1-C2	120.00
C10-C5-C6	120.00
C5-C6-C7	120.00
C6-C7-C8	119.20

For numbering of atom refer Fig.1 (a)

**Table 2.**  
**Definition of internal coordinates of 1,5-dinitronaphthalene**

No.(i)	Symbol	Type	Definition
<b>Stretching</b>			
1-6	$r_i$	C-H	C2-H14, C3-H15, C4-H16, C6-H20, C7-H21, C8-H22
7-17	$R_i$	C-C	C1-C2, C2-C3, C3-C4, C4-C10, C10-C9, C9-C1, C10-C5, C5-C6, C6-C7, C7-C8, C8-C9
18-19	$Q_i$	C-N	C1-N11, C5-N17
20-23	$P_i$	N-O	N11-O12, N11-O13, N17-O18, N17-O19
<b>Bending</b>			
24-29	$\beta_i$	Ring1	C1-C2-C3, C2-C3-C4, C3-C4-C10, C4-C10-C9, C10-C9-C1, C9-C1-C2
30-35	$\beta_i$	Ring2	C10-C5-C6, C5-C6-C7, C6-C7-C8, C7-C8-C9, C8-C9-C10, C9-C10-C5
36-47	$\alpha_i$	CCH	C1-C2-H14, C3-C2-H14, C2-C3-H15, C4-C3-H15, C3-C4-H16, C10-C4-H16, C5-C6-H20, C7-C6-H20, C6-C7-H21, C8-C7-H21, C7-C8-H22, C9-C8-H22
48-51	$\gamma_i$	CCN	C2-C1-N11, C9-C1-N11, C10-C5-N17, C6-C5-N17
52-55	$\delta_i$	CNO	C1-N11-O12, C1-N11-O13, C5-N17-O18, C5-N17-O19
56-57	$\delta_i$	ONO	O12-N11-O13, O18-N17-O19
<b>Out-of-plane bending</b>			
58-63	$\omega_i$	C-H	H14-C2-C1-C3, H15-C3-C2-C4, H16-C4-C3-C10, H20-C6-C7-C5, H21-C7-C8-C6, H22-C8-C9-C7
64-65	$\psi_i$	C-N	N11-C1-C2-C9, N17-C5-C10-C6
<b>Torsion</b>			
66-71	$t_i$	$\tau$ Ring 1	C1-C2-C3-C4, C2-C3-C4-C10, C3-C4-C10-C9, C4-C10-C9-C1, C10-C9-C1-C2, C9-C1-C2-C3
72-77	$t_i$	$\tau$ Ring 2	C10-C5-C6-C7, C5-C6-C7-C8, C6-C7-C8-C9, C7-C8-C9-C10, C8-C9-C10-C5, C9-C10-C5-C6
78-79	$t_i$	$\tau$ C-NO <sub>2</sub>	C1-N11-O12-O13, C5-N17-O18-O19
80-81	$t_i$	Butterfly	C8-C9-C10-C4, C1-C9-C10-C5

For numbering of atom refer Fig. 1.

**Table 3**

Definition of local symmetry coordinates and values of corresponding scale factors for the refined 6-311+G(d,p) and 6-311++G(d,p) force fields for 1,5-dinitronaphthalene.

No	Symbol	Definition	Scale factors used in the calculation	
			6-311+G(d,p)	6-311++G(d,p)
1-6	CH	$r_{11}, r_{12}, r_{13}, r_{14}, r_{15}, r_{16}$	0.912	0.926
7-17	CC	$R_{11}, R_{12}, R_{13}, R_{14}, R_{15}, R_{16}, R_{17}, R_{18}, R_{19}, R_{20}, R_{21}, R_{22}, R_{23}, R_{24}, R_{25}, R_{26}, R_{27}$	0.902	0.917
18-19	CN	$Q_{18}, Q_{19}$	0.902	0.917
20-21	NO <sub>2</sub> ss	$(P_{20}+P_{21})/\sqrt{2}, (P_{22}+P_{23})/\sqrt{2}$	0.902	0.917
22-23	NO <sub>2</sub> ass	$(P_{20}-P_{21})/\sqrt{2}, (P_{22}-P_{23})/\sqrt{2}$	1.003	1.023
24	R1 trig	$(\beta_{20}-\beta_{21}+\beta_{22}-\beta_{23}+\beta_{24}-\beta_{25})/\sqrt{6}$	0.986	0.966
25	R1 sym	$(-\beta_{20}-\beta_{21}+2\beta_{22}-\beta_{23}-\beta_{24}+2\beta_{25})/\sqrt{12}$	0.986	0.966
26	R1 asym	$(\beta_{20}-\beta_{21}+\beta_{22}-\beta_{23})/2$	0.986	0.966
27	R2 trig	$(\beta_{20}-\beta_{21}+\beta_{22}-\beta_{23}+\beta_{24}-\beta_{25})/\sqrt{6}$	0.986	0.966
28	R2 sym	$(-\beta_{20}-\beta_{21}+2\beta_{22}-\beta_{23}+\beta_{24}-2\beta_{25})/\sqrt{12}$	0.986	0.966
29	R2 asym	$(\beta_{20}-\beta_{21}+\beta_{22}-\beta_{23})/2$	0.986	0.966
30-35	bCH	$(\alpha_{30}-\alpha_{31})/\sqrt{2}, (\alpha_{31}-\alpha_{32})/\sqrt{2}, (\alpha_{32}-\alpha_{33})/\sqrt{2}, (\alpha_{33}-\alpha_{34})/\sqrt{2}, (\alpha_{34}-\alpha_{35})/\sqrt{2}, (\alpha_{35}-\alpha_{36})/\sqrt{2}$	0.942	0.976
36-37	bCN	$(\gamma_{36}-\gamma_{37})/\sqrt{2}, (\gamma_{37}-\gamma_{38})/\sqrt{2}$	0.961	0.958
38-39	NO <sub>2</sub> twist	$(\delta_{38}+\delta_{39})/\sqrt{2}, (\delta_{39}-\delta_{40})/\sqrt{2}$	0.916	0.904
40-41	NO <sub>2</sub> rock	$(\delta_{38}-\delta_{39})/\sqrt{2}, (\delta_{39}-\delta_{40})/\sqrt{2}$	0.916	0.904
42-43	NO <sub>2</sub> sciss	$(2\delta_{38}-\delta_{39}-\delta_{40})/\sqrt{6}, (2\delta_{39}-\delta_{38}-\delta_{40})/\sqrt{6}$	0.916	0.904
44-49	ωCH	$\omega_{41}, \omega_{42}, \omega_{43}, \omega_{44}, \omega_{45}, \omega_{46}, \omega_{47}$	0.966	0.959
50-51	ωCN	$\omega_{48}, \omega_{49}$	0.939	0.987
52	tR1 trig	$(\tau_{50}-\tau_{51}+\tau_{52}-\tau_{53}+\tau_{54}-\tau_{55})/\sqrt{6}$	0.934	0.895
53	tR1 sym	$(\tau_{50}-\tau_{51}+\tau_{52}-\tau_{53})/\sqrt{2}$	0.934	0.895
54	tR1 asym	$(-\tau_{50}+2\tau_{51}-\tau_{52}-\tau_{53}+2\tau_{54}-\tau_{55})/\sqrt{12}$	0.934	0.895
55	tR2 trig	$(\tau_{52}-\tau_{53}+\tau_{54}-\tau_{55}+\tau_{56}-\tau_{57})/\sqrt{6}$	0.934	0.895
56	tR2 sym	$(\tau_{52}-\tau_{53}+\tau_{54}-\tau_{55})/\sqrt{2}$	0.934	0.861
57	tR2 asym	$(-\tau_{52}+2\tau_{53}-\tau_{54}-\tau_{55}+2\tau_{56}-\tau_{57})/\sqrt{12}$	0.934	0.895
58-59	NO <sub>2</sub> wag	$\tau_{58}, \tau_{59}$	0.831	0.831
60	Butterfly	$(\tau_{60}-\tau_{61})/\sqrt{2}$	0.831	0.831

These symbols are used for description of normal modes by TED in Table 4. The internal coordinates used here are in Table 2 Table 4

**Table 4**

Assignment of fundamental vibrations of 1,5-dinitronaphthalene by normal mode analysis based calculations using B3LYP/6-311+G\*\* force field

Symm species	C	Observed fundamentals (cm <sup>-1</sup> )		TED (%) among types of coordinates	
		FTIR	Raman	Unscaled B3LYP/6-311+G(d,p)	
A'		3100 (w)		3351	vCH(99)
A'			3084 (w)	3350	vCH(98)
A'			3064 (vw)	3289	vCH(98)
A'		3050 (vw)		3288	vCH(97)
A'		2992 (w)		3284	vCH(96)
A'		2988 (vw)		3181	vCH(95)
A'		1884 (vw)		1948	vCC(94)
A'		1805 (s)		1787	NC <sub>2</sub> ss(92)
A'		1590 (w)		1730	vCC(90), bCH
A'			1567 (s)	1691	NC <sub>2</sub> ss(92)
A'			1552 (w)	1697	vCC(89), bCH(10)
A'		1519 (vs)		1625	vCC(89), bCN(11)
A'		1490 (vw)		1589	vCC(88), bCN(10)
A'		1475 (vw)		1571	vCN(84), bCN(10)
A'			1459 (w)	1552	vCN(81), vCC(13)
A'			1420 (vs)	1507	vCC(80), R1 sym(14)
A'			1352 (vs)	1483	NC <sub>2</sub> ss(84)
A'		1347 (s)		1426	NC <sub>2</sub> ss(84)
A'		1297 (w)		1374	vCC(82), R2 asym(13)
A'			1280 (vw)	1355	vCC(81), R2 trig(11)
A'		1256 (vw)		1388	vCC(83), R2 sym(15)
A'		1231 (ms)		1303	vCC(80), vCN(12)
A'		1208 (vw)		1277	vCC(81), R1 trig(12)
A'			1188 (w)	1235	bCH(79), vCC(19)
A'		1170 (w)		1235	bCH(79), R1 sym(17)
A'		1148 (w)		1209	bCH(78), vCC(13)
A'			1097 (w)	1152	bCH(77), R2 sym(19)
A'		1050 (w)		1101	bCH(76), R2 trig(13)
A'		1038 (w)		1087	bCH(77), R1 sym(12)
A'		1017 (w)		1060	R1 trig(36), vCC(23)
A'			992 (w)	1083	R1 sym(37), R1 sym(23)
A'		982 (vw)		1021	R2 sym(37), R2 sym(29)
A'			958 (w)	995	R2 trig(61), bCH
A'		890 (s)		926	bCN(60), vCC(23)
A'			825 (w)	846	R1 sym(61), R1 sym(24)
A'			803 (s)	838	bCN(59), R1 sym(21)
A'		791 (vs)		824	NC <sub>2</sub> sciss(61)
A'		752 (vs)		782	NC <sub>2</sub> sciss(59)
A'			729 (w)	762	R1 sym(61), R1 sym(21)
A'		571 (ms)		592	NC <sub>2</sub> rock(63)
A'			568 (w)	585	NC <sub>2</sub> rock(62)
A'		715 (vs)		744	NC <sub>2</sub> wag(71)
A'			691 (w)	718	vCH(61), tR1 sym(23)
A'			680 (vs)	682	NC <sub>2</sub> wag(73)
A'		648 (w)		669	vCH(60), tR1 trig(27)
A'		624 (w)		643	vCH(59), bCH(23)
A'			618 (vw)	639	vCH(61), tR1 sym(21)
A'			601 (vw)	632	vCH(59), tR2 sym(23)
A'			594 (vw)	613	vCH(58), tR2 sym(17)
A'			540 (vw)	553	vCN(60), tR1 trig(19)
A'		530 (vw)		545	vCN(57)
A'			480 (vw)	503	tR1 trig(57), tR1 sym(27)
A'		471 (vw)		488	tR1 sym(59), tR1 trig(37)
A'			458 (vw)	484	tR2 sym(51), tR2 sym(31)
A'		456 (vw)		457	tR1 sym(60), tR1 trig(26)
A'		393 (w)		410	tR1 trig(56), tR2 sym(27)
A'		385 (w)		381	tR2 sym(53), tR2 trig(23)
A'		187 (w)		206	NC <sub>2</sub> (twist) (59)
A'		167 (w)		190	NC <sub>2</sub> (twist) (57)
A'			156 (w)	177	Butterfly(36)

Abbreviations :ss-symmetric stretching; ass-antisymmetric stretching; b-bending; R-Ring; t-torsion; ω-

out-of-plane bending; vs – very strong; s – strong; ms – medium strong; m – medium; w – weak; vw-very weak.

**Table 5.**

Calculated energy values of title compound by B3LYP/6-311++G(d,p) method.

Basis set	B3LYP/6-311++G(d,p)
$E_{ground}(eV)$	-6.9795
$E_{LUMO}(eV)$	-2.8564
Ionization potential	6.9795
Electron affinity	2.8564
Energy gap(eV)	4.1231
Electronegativity	4.9180
Chemical potential	-4.9180
Chemical hardness	2.0616
Chemical softness	0.2425
Electrophilicity index	5.8660

**Table 6.**

The values of calculated dipole moment  $\mu(D)$ , polarizability ( $\alpha_0$ ), first order hyperpolarizability ( $\beta_{tot}$ ) components of DNN

Parameters	B3LYP/6-311++G(d,p)	Parameters	B3LYP/6-311++G(d,p)
$\mu_x$	-2.4592	$\beta_{xxx}$	-1446.0811
$\mu_y$	0.2617	$\beta_{xxy}$	-211.6654
$\mu_z$	-0.1392	$\beta_{xyy}$	-22.3545
$\mu(D)$	2.4770	$\beta_{yyy}$	102.806
$\alpha_{xx}$	302.0000	$\beta_{zxx}$	-743.514
$\alpha_{xy}$	24.1296	$\beta_{xyx}$	-65.6032
$\alpha_{yy}$	119.6955	$\beta_{zyy}$	65.0575
$\alpha_{xz}$	53.6948	$\beta_{xzz}$	-269.1156
$\alpha_{yz}$	28.8030	$\beta_{yzz}$	-2.5045
$\alpha_{zz}$	194.6897	$\beta_{zzz}$	128.764
$\alpha_0$ (e.s.u)	$3.0449 \times 10^{-23}$	$\beta_{tot}$ (e.s.u)	$15.7740 \times 10^{-30}$
$\Delta\alpha$ (e.s.u)	$8.1010 \times 10^{-23}$		

**Table 7**

Temperature dependence of thermodynamic properties of DNN at B3LYP /6-311++G(d,P)

T(K)	(J/ mol K)	(J/ mol K)	(kJ/ mol)
100	108.479	357.641	7.234
200	175.723	453.221	21.408
298.15	243.456	536.09	42.000
300	244.693	537.599	42.451
400	306.735	616.735	70.108
500	357.512	690.851	103.417
600	397.545	759.719	141.251
700	429.049	823.461	182.642
800	454.169	882.454	226.848
900	474.528	937.163	273.318
1000	491.273	988.054	321.634

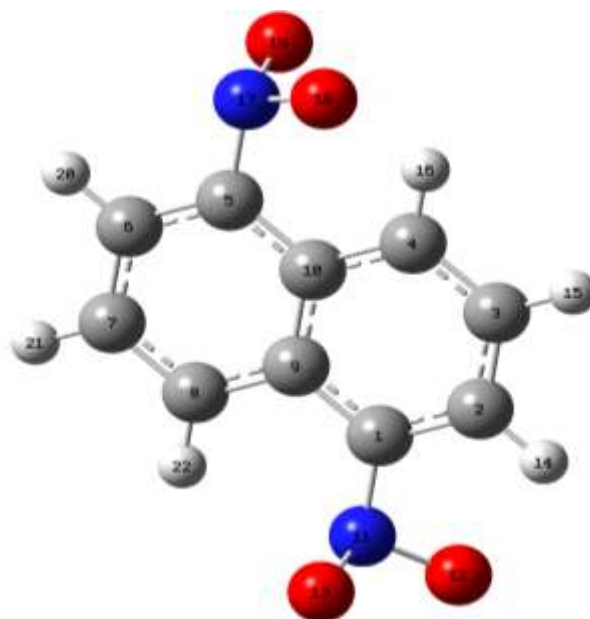


Fig.1 Molecular Structure of 1,5-dinitronaphthalene

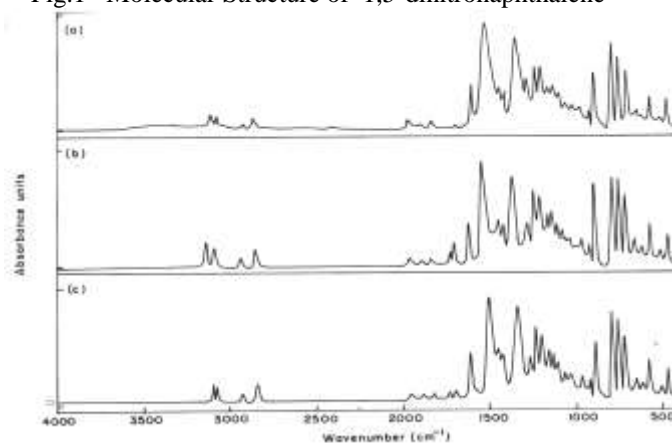


Fig. 2 Comparison of Observed and Calculated infrared spectra of 1,5-dinitro naphthalene (a)Observed in Solid Phase (b) Calculated with B3LYP /6-311+G(d,p) (c) Calculated with B3LYP /6-311++G(d,p)

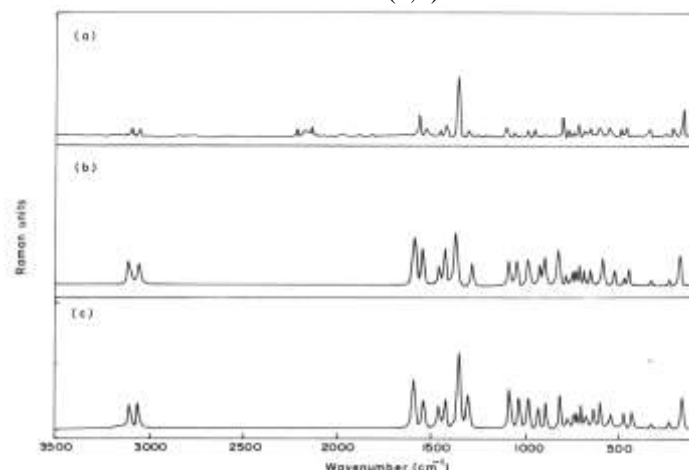


Fig. 3 Comparison of Observed and Calculated Raman spectra of 1,5-dinitronaphthalene (a)Observed in Solid Phase (b) Calculated with B3LYP /6-311+G(d,P) (c) Calculated with B3LYP /6-311++G(d,P).

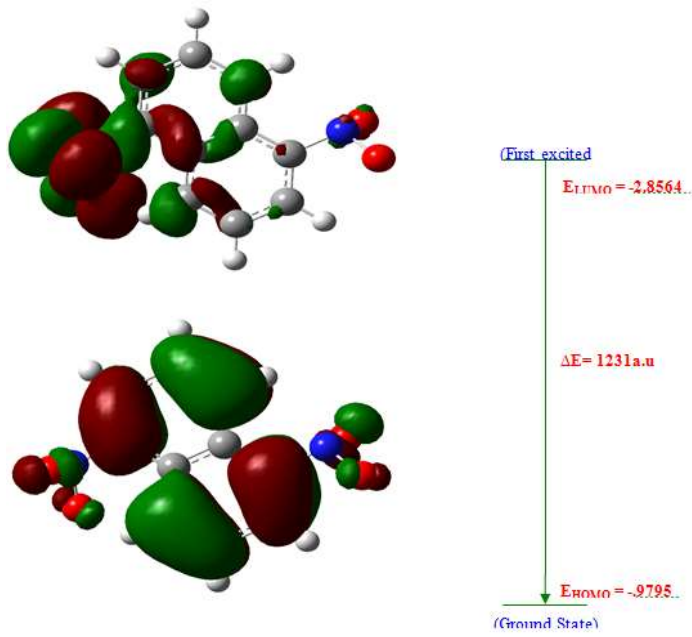


Fig. 4: HOMO-LUMO Plot of 1,5-Dinitronaphthalene.

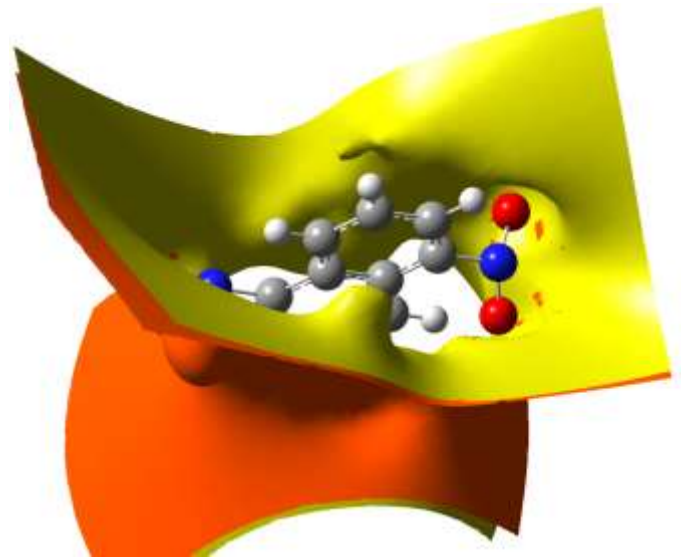


Fig 7. The contour map of the electrostatic potential surface of 1,5-Dinitronaphthalene.

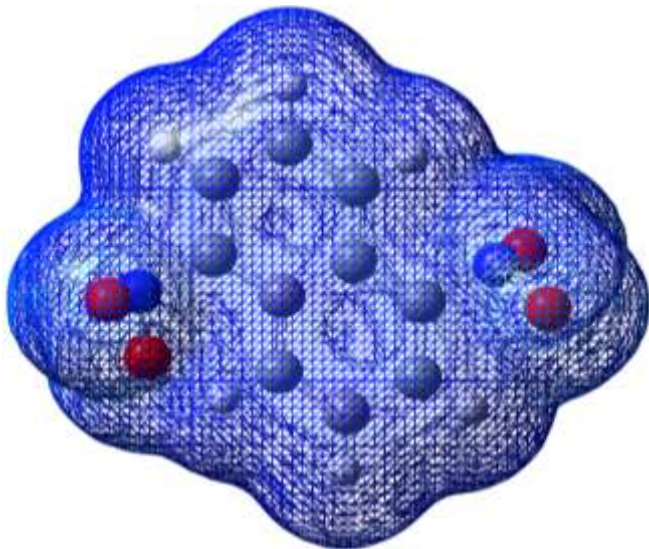


Fig 5. The total electron density surface of 1,5-Dinitronaphthalene.

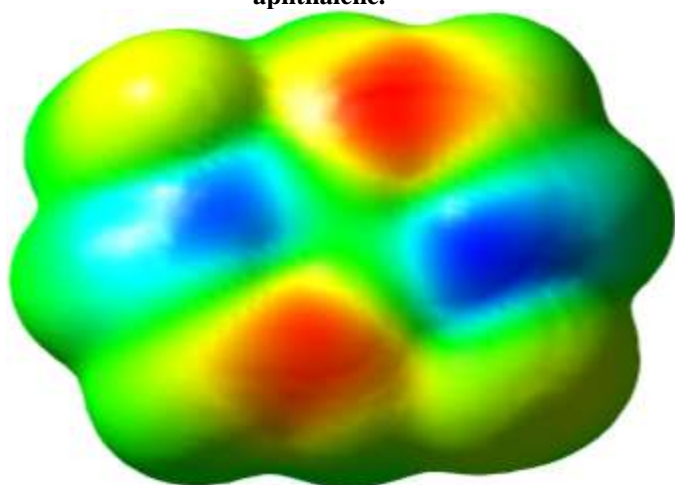


Fig 6. The molecular electrostatic potential surface of 1,5-Dinitronaphthalene

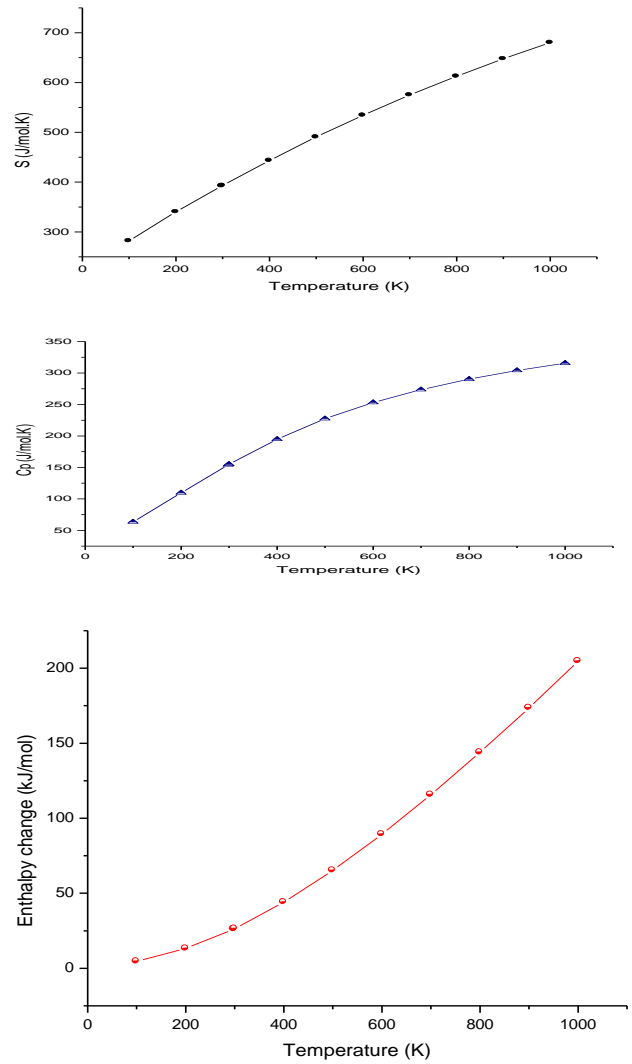


Fig 8 : The effect of temperature on entropy (S), heat capacity (Cp) & enthalpy change (ΔH0) of 1,5-Dinitronaphthalene.